

A New Computational Model to Predict Breakdown Pressures in Cased and Perforated Wells in Unconventional Reservoirs

Mohammed Kurdi *
Saudi Aramco
Saudi Arabia
Kurdms0b@gmail.com

Hamid Roshan
UNSW
UNSW, Kensington NSW
H.Roshan@unsw.edu.au

SUMMARY

Unconventional shale reservoirs are characterised by their extreme low permeabilities and their high in-situ stresses. Multi-stage hydraulic fracturing therefore plays a key role in developing such reservoirs. However, depending on the in-situ stress magnitude and/or regime, breakdown pressures can be too extreme to achieve, given the available surface horsepower capabilities. The local principal stresses surrounding perforation tunnels dictate the required breakdown pressure to induce enough stress to exceed the rock tensile strength.

This paper presents a newly developed model to predict the breakdown pressures in cased and perforated wells. Given an arbitrary azimuth and inclination of the wellbore and the in-situ stress magnitude/regime, the model calculates the local stresses around the perforations and consequently predicts the perforations' breakdown pressure and the initial fracture plane orientation.

The results from the model indicate as to which perforation initiates first, creating a mini-fracture that extends to create a dominant fracture. This dominant fracture would be the only fracture extending, due to the induced stress shadowing on other mini-fractures and increasing the respective in-situ principal stresses. The model also aids cluster and well placement for highly deviated wells to better identify sweet spots where breakdown pressures are minimal, resulting in maximum hydrocarbon accumulations possible. If the perforations clusters are placed in zones with extreme local principal stresses, the near wellbore fracture widths would be too small to admit any proppant, leading to early proppant screenout. The results from the model shows a critical perforation phasing angle that should be avoided, as the local principal stresses maximise, increasing breakdown pressures.

The model aims to advance the current understanding of fracture initiation in highly deviated wells in shale reservoirs. It can also assist engineers to better select sweet spots for well and cluster placement to avoid excessive breakdown pressures and/or potential early proppant screenout.

Key words: shale, hydraulic fracturing, unconventional.

INTRODUCTION

Background

Unconventional shale reservoirs are typically characterised by their low permeabilities and high in-situ stresses. To efficiently develop these reservoirs, oil and gas operators drill and complete horizontal wells within the target shale to maximize contact with the reservoir. Then, multi-stage hydraulic fracturing is applied to stimulate a number of clusters across the target zone. Once the clusters are perforated and hydraulic fracturing is applied, these clusters initiate transverse fractures, creating a fracture network that is required for reservoir depletion. At each cluster, the pressure delivered from the surface pumping units is exerted on the rock until the breakdown pressure is achieved. If the breakdown pressure is not achieved at a given cluster, there will be no induced fractures and consequently no production.

Breakdown Pressure in the Literature

There are several studies found in the literature that investigate and calculate formation breakdown. Rickman et al. (2008) introduced the Brittleness Index (BI) and correlated it to rock breakdown. This index incorporates the measured Young's Modulus and Poisson's Ratio along the lateral wellbore via logs and cores to determine how brittle the rock is. This however does not consider the local stresses around the perforations, the different faulting stress regimes and the wellbore trajectory which can change the rock failure response to hydraulic fracturing. Khan et al. (2016) took into account the faulting stress regimes and the stress magnitudes in calculating the breakdown pressure along horizontal wells. Their model uses Hubbert & Willis (1957) method that modified the original Kirsch solution in 1898. The breakdown pressure for vertical wells is given as follows:

$$P_b = 3\sigma_{hmin} - \sigma_{Hmax} - \alpha P_p + T_0 \quad (1)$$

Equation (1) was modified to consider horizontal wells drilled towards the minimum horizontal stress (σ_h), a typical lateral direction for shale wells. The modified equations for different faulting stress regimes are shown in Table 1. This model however uses the assumption that the wellbore is an open hole and the local stresses around the wellbore are those surrounding open-hole wells. This could be used as a solution for a sliding sleeve system where a completion is run in an uncemented wellbore with sleeves that open

without the need for perforations to make contact with the rock. However, Plug and Perf wells involve running a casing and perforation notches are created, changing the local stresses surrounding the wellbore.

Stress Regime	Breakdown Pressure	$\Delta\sigma$
Normal Stress Regime ($\sigma_v > \sigma_{HMax} > \sigma_{hmin}$)	$2\sigma_{HMax} - \Delta\sigma - \alpha P_p + T_0$	$\sigma_v - \sigma_{HMax}$
Strike-slip Stress Regime ($\sigma_{HMax} > \sigma_v > \sigma_{hmin}$)	$2\sigma_v - \Delta\sigma - \alpha P_p + T_0$	$\sigma_{HMax} - \sigma_v$
Reverse Stress Regime ($\sigma_{HMax} > \sigma_{hmin} > \sigma_v$)	$2\sigma_v - \Delta\sigma - \alpha P_p + T_0$	$\sigma_{HMax} - \sigma_v$

Table 1: Breakdown pressures for a horizontal well drilled against σ_h at different stress regimes (Khan et al. 2016)

Hossain et al. (2000) proposed a model to predict the breakdown pressure for different faulting stress regimes and wellbore trajectories for cased and perforated wells. The method involves the same Kirsch solution while considering perforation notches. For a horizontal well oriented towards the minimum horizontal stress, two cases are considered: A perforation on top of the wellbore (Pw0) and a perforation on the side of the wellbore (Pw90)

$$P_{w0} = \frac{1}{4} \{9\sigma_H - \sigma_h - 3\sigma_v + 2\nu(\sigma_v - \sigma_H)\} \quad (2)$$

$$P_{w90} = \frac{1}{4} \{9\sigma_v - \sigma_h - 3\sigma_H + 2\nu(\sigma_v - \sigma_H)\} \quad (3)$$

The model assumes the pore pressure and the rock tensile strength are zero as their exact value are difficult to determine at the design stage. The model also assumes that the pore pressure and the tensile strength values counterbalance each other in terms of magnitude as the tensile strength is negative in value. However, tensile strengths of sedimentary rocks are very low compared to the pore pressure at targeted depths. In addition, the model assumes a perfect hydraulic communication between the wellbore and the perforations due to a micro-annulus existing between the cement and the rock. However, there would be no perfect hydraulic communication if there is good bonding cement, indicated by the Cement Bond Log (CBL). Also, the model only assumes that breakdown occurs at the base of the perforation wall close to the wellbore and ignores breakdown at the tip of the perforation wall. To consider the tensile strength and the pore pressure, a model was constructed using MATLAB software program. The following expressions are deduced:

$$P_{w0} = \frac{1}{4} * [9\sigma_H - \sigma_h - 3\sigma_v + 2\nu(\sigma_v - \sigma_H) + T_0] \quad (4)$$

$$P_{w90} = \frac{1}{4} * [9\sigma_v - \sigma_h - 3\sigma_H + 2\nu(\sigma_H - \sigma_v) + T_0]$$

STUDY OBJECTIVE, METHODOLOGY AND RESULTS

The main objective of this study is to investigate the physics behind fracture initiation of cased and perforated wells in extremely tight reservoirs. This involves building a computational model to calculate the breakdown pressure for an inclined well at given azimuth and inclination angles. The developed model considers the in-situ stress magnitudes and faulting stress regimes to analyse local stresses around the perforations to predict the fracture initiation pressure and orientation. Fracture propagation is outside of the study scope.

Development of Proposed Model: Stress Distribution around the Wellbore

The stresses acting on the rock deposited at a given depth are: The vertical (overburden) stress (SV), the maximum horizontal stress (SH) and the minimum horizontal stress (Sh). These are called in-situ stresses, or far field stresses, and depending on their magnitudes, they define the faulting stress regimes as shown in Fig. 1. When a wellbore is drilled into the rock and a mud pressure is exerted, the wellbore becomes a free surface and stresses are perturbed near the wellbore wall. As shown in Fig. 2, assuming the rock is elastic and isotropic, the local stresses (S_1 and S_3) converge near the wellbore wall at the azimuth of S_{hmin} , creating a high compressive area that is prone to drilling breakouts. The stresses diverge in the azimuth of S_{Hmax} , creating a low compressive area that is prone to drilling tensile failure. Therefore, these local stresses need to be deduced from the in-situ stresses to analyse the near wellbore area. To take the effective stress into account in the calculation, the pore pressure needs to be subtracted from the in-situ stress ($\sigma = S - P_p$).

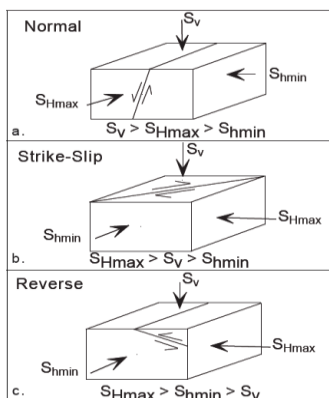


Figure 1: Anderson faulting stress regime classification of in-situ stresses (Zoback, 2010)

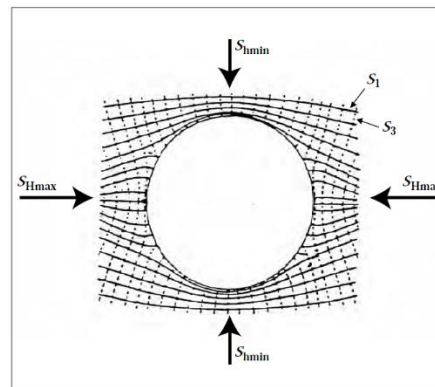


Figure 2: Stress perturbation due to drilled wellbore showing high local stress compression at the azimuth of S_{hmin} and low compression at the azimuth of S_{Hmax} (Zoback, 2010)

Transforming In-Situ Stresses to Cartesian Stresses

Bradley (1979) provided a full solution for this problem. Fjaer et al. (2008) built on the full solution and provided simple transformation formula from in-situ to local stresses. The formula are modified here to take the effective stress concept into account. A new coordinate system is introduced. As shown in Fig. 3, the z' axis is to be aligned with σ_v , y' to be aligned with σ_h and x' to be aligned with σ_H . Then, another coordinate system is introduced as shown in Fig. 4, the z axis is aligned with the wellbore axis, the x axis is aligned with the lowermost radial hole direction and the y axis is horizontal. Depending on the wellbore inclination angle i and azimuth angle a , the coordinate system (x',y',z') is transformed to the coordinate system (x,y,z) by rotating a around the z' axis and then rotating i around the y axis.

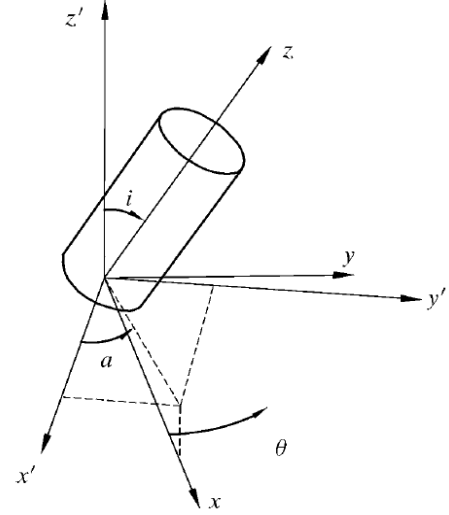
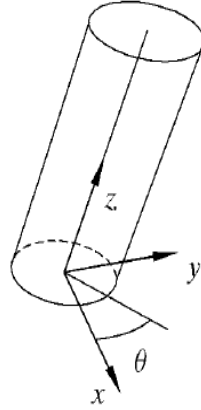
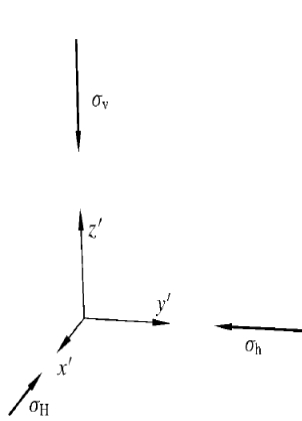


Figure 3: deviated well coordinate system (Fjaer et al. 2008)

Figure 4: Geometry of transformed coordinate system (Fjaer et al. 2008)

The resultant Cartesian stresses σ_x , σ_y and σ_z and the shear stresses are given as follows:

$$\begin{aligned}
 \sigma_x^o &= l_{xx'}^2 \sigma_H + l_{xy'}^2 \sigma_h + l_{xz'}^2 \sigma_v \\
 \sigma_y^o &= l_{yx'}^2 \sigma_H + l_{yy'}^2 \sigma_h + l_{yz'}^2 \sigma_v \\
 \sigma_z^o &= l_{zx'}^2 \sigma_H + l_{zy'}^2 \sigma_h + l_{zz'}^2 \sigma_v \\
 \tau_{xy}^o &= l_{xx'} l_{yx'} \sigma_H + l_{xy'} l_{yy'} \sigma_h + l_{xz'} l_{yz'} \sigma_v \\
 \tau_{yz}^o &= l_{yx'} l_{zx'} \sigma_H + l_{yy'} l_{zy'} \sigma_h + l_{yz'} l_{zz'} \sigma_v \\
 \tau_{zx}^o &= l_{zx'} l_{xx'} \sigma_H + l_{zy'} l_{xy'} \sigma_h + l_{zz'} l_{xz'} \sigma_v
 \end{aligned} \tag{5}$$

Where,

$$\begin{aligned}
 l_{xx'} &= \cos a \cos i, & l_{xy'} &= \sin a \cos i, & l_{xz'} &= -\sin i \\
 l_{yx'} &= -\sin a, & l_{yy'} &= \cos a, & l_{yz'} &= 0 \\
 l_{zx'} &= \cos a \sin i, & l_{zy'} &= \sin a \sin i, & l_{zz'} &= \cos i
 \end{aligned} \tag{6}$$

Transforming Cartesian Stresses to Cylindrical Stresses

To analyse the stresses at the wellbore wall, it is more convenient to transform the (x,y,z) coordinate system to the cylindrical polar coordinate system (r, θ, z) . As shown in Fig. 5, r represents the distance from the centre of the wellbore. θ is the angle relative to the x axis and z is the distance along the wellbore axis. The radial stress (σ_r), the tangential stress (σ_θ), the axial stress (σ_z) and the shear stresses are deduced as follows where R_w is the wellbore radius, ΔP is the difference between wellbore pressure and pore pressure and ν is poisson's ratio.

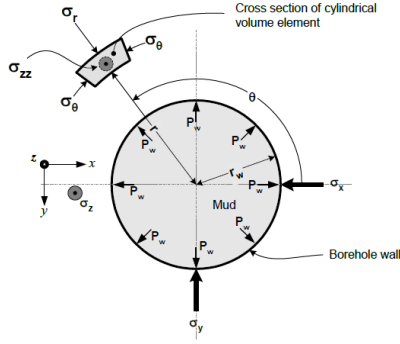


Figure 5: cylindrical polar coordinate system (Chen, 2016)

$$\begin{aligned}
 \sigma_r &= \frac{\sigma_x^o + \sigma_y^o}{2} \left(1 - \frac{R_w^2}{r^2}\right) + \frac{\sigma_x^o - \sigma_y^o}{2} \left(1 + 3\frac{R_w^4}{r^4} - 4\frac{R_w^2}{r^2}\right) \cos 2\theta + \tau_{xy}^o \left(1 + 3\frac{R_w^4}{r^4} - 4\frac{R_w^2}{r^2}\right) \sin 2\theta + \Delta P \frac{R_w^2}{r^2} \\
 \sigma_\theta &= \frac{\sigma_x^o + \sigma_y^o}{2} \left(1 + \frac{R_w^2}{r^2}\right) - \frac{\sigma_x^o - \sigma_y^o}{2} \left(1 + 3\frac{R_w^4}{r^4}\right) \cos 2\theta - \tau_{xy}^o \left(1 + 3\frac{R_w^4}{r^4}\right) \sin 2\theta - \Delta P \frac{R_w^2}{r^2} \\
 \sigma_z &= \sigma_z^o - \nu_{fr} \left[2(\sigma_x^o - \sigma_y^o) \frac{R_w^2}{r^2} \cos 2\theta + 4\tau_{xy}^o \frac{R_w^2}{r^2} \sin 2\theta \right] \\
 \tau_{r\theta} &= \frac{\sigma_y^o - \sigma_x^o}{2} \left(1 - 3\frac{R_w^4}{r^4} + 2\frac{R_w^2}{r^2}\right) \sin 2\theta \\
 &\quad + \tau_{xy}^o \left(1 - 3\frac{R_w^4}{r^4} + 2\frac{R_w^2}{r^2}\right) \cos 2\theta \\
 \tau_{\theta z} &= (-\tau_{xz}^o \sin \theta + \tau_{yz}^o \cos \theta) \left(1 + \frac{R_w^2}{r^2}\right) \\
 \tau_{rz} &= (\tau_{xz}^o \cos \theta + \tau_{yz}^o \sin \theta) \left(1 - \frac{R_w^2}{r^2}\right)
 \end{aligned} \tag{7}$$

Stress Distribution around Perforations

To analyse the stress distribution around perforations, certain assumptions are made: the rock is elastic and isotropic, there is good cement bonding between the hole and the casing, and the perforations are cylindrical in shape. The same transformation from Cartesian to cylindrical coordinate system previously applied to the wellbore is applied here. Taken the radius of investigation as r_p (at the perforation wall), the following equations define the new cylindrical coordinate system at perforations where the p subscript refer to those stresses belonging to perforations:

$$\begin{aligned}
 \sigma_{rp} &= \Delta P \\
 \sigma_{\theta p} &= \sigma_z + \sigma_\theta - 2(\sigma_z - \sigma_\theta) \cos 2\theta_p - 4\tau_{z\theta} \sin 2\theta_p - \Delta P \\
 \sigma_{zp} &= \sigma_r - \nu \left(2(\sigma_z - \sigma_\theta) \cos 2\theta_p + 4\tau_{z\theta} \sin 2\theta_p \right) \\
 \tau_{r\theta p} &= \tau_{rzp} = 0 \\
 \tau_{\theta zp} &= 2(-\tau_{rz} \sin \theta_p + \tau_{r\theta} \cos \theta_p)
 \end{aligned} \tag{8}$$

As shown in Fig. 6, θ_p is the angle around the perforation hole with reference to top of perforation. As seen from equations (7), two of the shear stresses are zero while the third shear stress is nonzero. This means that the normal stresses are not principals and by applying the Mohr circle concept, the prin $\sigma_1 = \sigma_{rp}$,

$$\begin{aligned}
 \sigma_2 &= 0.5\{(\sigma_{\theta p} + \sigma_{zp}) + ((\sigma_{\theta p} - \sigma_{zp})^2 + 4\tau_{\theta zp})^{1/2}\}, \\
 \sigma_3 &= 0.5\{(\sigma_{\theta p} + \sigma_{zp}) - ((\sigma_{\theta p} - \sigma_{zp})^2 + 4\tau_{\theta zp})^{1/2}\}.
 \end{aligned} \tag{9}$$

To initiate a fracture, the following failure criteria applies:

$$\sigma_3 < -TS$$

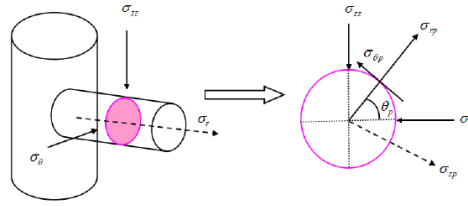


Figure 6: perforation cylindrical polar coordinate system (Li et al., 2015)

Results and Discussion

Normal faulting stress regime

The following rock properties and wellbore trajectories were used as input parameters in the model:

- Inclination angle = 90 degrees
- Azimuth angle = 0 to 180 degrees
- Target depth = 10,000 feet
- Tensile strength = 500 psi
- Poisson's ratio = 0.25
- Overburden gradient = 1.1 psi/ft
- Maximum horizontal stress gradient = 1 psi/ft
- Minimum horizontal stress gradient = 0.9 psi/ft
- Pore pressure gradient = 0.6 psi/ft
- Wellbore diameter = 4.5 inches

The maximum horizontal stress (SH) direction defines the wellbore azimuth as a reference and the azimuth angle is taken from 0 degrees (direction of SH) to 180 degrees (direction of Sh). The in-situ stress coordinate system can be transformed to the Cartesian coordinate system using equations (5) and (6). Using equations (7), the cylindrical coordinate system can be calculated. For a horizontal well oriented towards Sh and the value of r taken from the wellbore radius (2.25 inches) to a typical perforation penetration depth (18 inches), the resultant cylindrical stress distribution is shown in Fig. 7 (perforation on top/bottom of wellbore) and Fig. 8 (perforation on sides of wellbore). It can be shown that local stresses converge to the far field in-situ stresses at the depth of penetration. Stresses exerted on the rock by the cement is ignored in this model. However, future work will consider the stresses exerted by a combination of the fully hydrated cement and the respective stress relaxation rate on the rock face. For this model, the radius of investigation will be at the tip of the perforation tunnel as the induced stress from the cement will not influence the local stresses at the tip due to the long penetration depth.

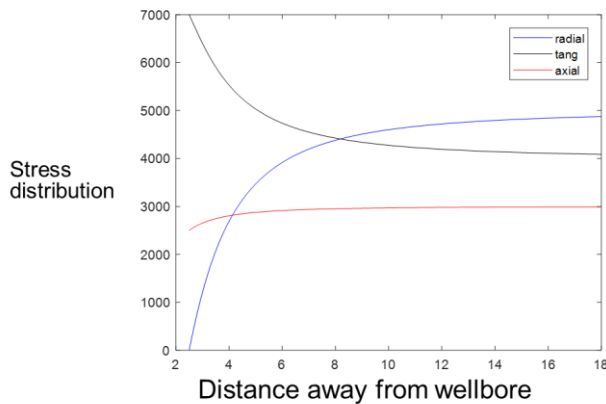


Figure 7: Cylindrical stress distribution for a top/bottom perforation

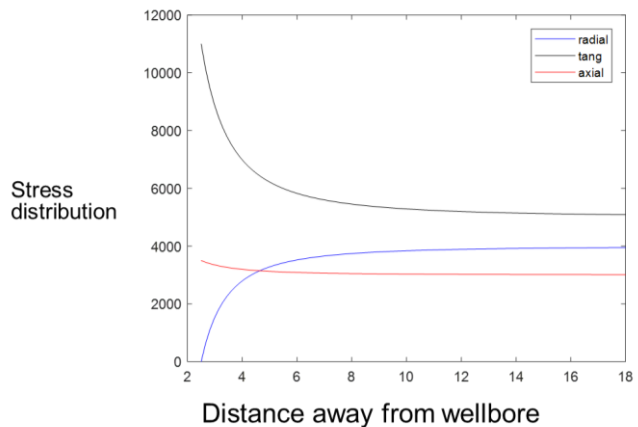


Figure 8: Cylindrical stress distribution for a side perforation

The stress distribution around the perforation can be determined at different θ_p using equations (8). The principal stresses and the tensile failure criteria can be applied using equations (9). The only unknown parameter in the system is the breakdown pressure. Fig. 9 shows the breakdown pressure distribution at different wellbore azimuth angles (0 degrees corresponding to SH orientation) and perforation angles (0 degrees corresponding to a perforation on top of the wellbore). There are two extreme cases:

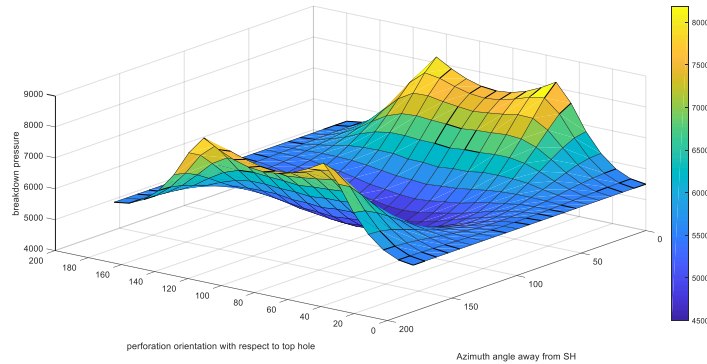


Figure 9: Breakdown pressure distribution for a normal faulting stress regime

1. Minimum breakdown for a well oriented towards Sh (90 degrees) and side perforations (90 degree perforation phasing angle)

Sh and SV are the only acting stresses around the perforation as shown in Fig. 10. The angle of failure θ_p is 90 degrees and the corresponding equation is:

$$P_b = 3*Sh - SV + T_0 \quad (10)$$

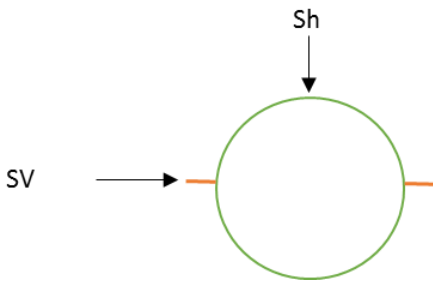


Figure 10: Minimum breakdown pressure case where perforation is on the sides and wellbore is 90 degree azimuth

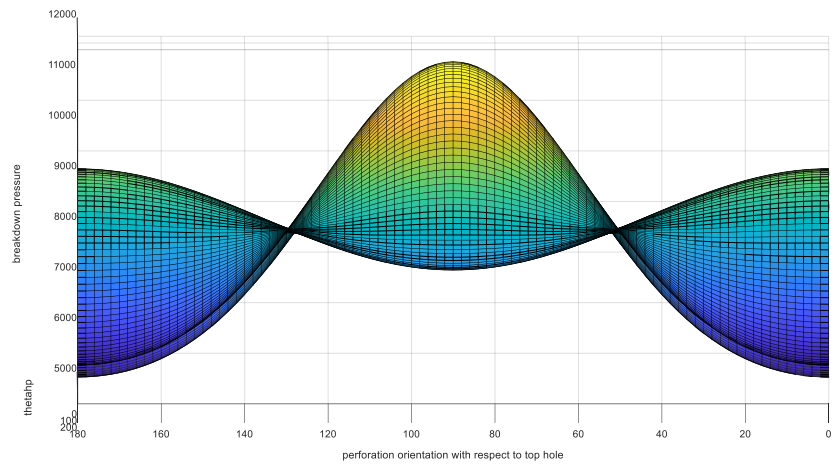


Figure 11: Maximum breakdown pressure case for normal faulting stress regime

2. Maximum breakdown for a well oriented towards SH (0 degrees) and 52 degree perforation phasing angle

Fig. 11 shows the breakdown pressure distribution for different perforation phasing angles. The range of breakdown pressure distribution defines the angle around the perforation. The minimum breakdown pressure maximizes at around 52 degrees. This is the maximum breakdown pressure for all azimuth angles.

Strike-slip faulting stress regime

The following rock properties and wellbore trajectories were used as input parameters in the model:

- Inclination angle = 90 degrees
- Azimuth angle = 0 to 180 degrees
- Target depth = 10,000 feet
- Tensile strength = 500 psi
- Poisson's ratio = 0.25
- Overburden gradient = 1.1 psi/ft
- Maximum horizontal stress gradient = 1.2 psi/ft
- Minimum horizontal stress gradient = 0.9 psi/ft
- Pore pressure gradient = 0.6 psi/ft
- Wellbore diameter = 4.5 inches

The same computational procedure is applied. Fig. 12 shows the breakdown pressure distribution for different wellbore azimuth angles and perforation phasing angles. There are two extreme cases:

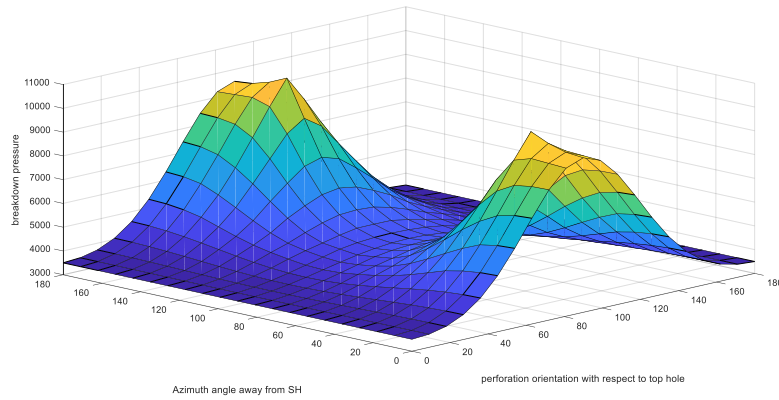


Figure 12: Breakdown pressure distribution for a strike-slip faulting stress regime

1. Minimum breakdown for a well with top perforations (0 degree perforation phasing angle)

At any given azimuth angles, the stresses acting on the system are the maximum and minimum horizontal stresses. The breakdown pressure is calculated as follows:

$$P_b = 3 * S_h - S_H + T_0 \quad (11)$$

2. Maximum breakdown for a well with side perforations (90 degree perforation phasing angle) at 40 degree wellbore azimuth angle
The non-zero shear stresses cause the minimum principal stress at the perforation wall to maximize at this azimuth angle, increasing the breakdown pressure.

Reverse faulting stress regime

The following rock properties and wellbore trajectories were used as input parameters in the model:

- Inclination angle = 90 degrees
- Azimuth angle = 0 to 180 degrees
- Target depth = 10,000 feet
- Tensile strength = 500 psi
- Poisson's ratio = 0.25
- Overburden gradient = 1.1 psi/ft
- Maximum horizontal stress gradient = 1.2 psi/ft
- Minimum horizontal stress gradient = 1.15 psi/ft
- Pore pressure gradient = 0.6 psi/ft
- Wellbore diameter = 4.5 inches

Fig. 13 shows the breakdown pressure distribution for different wellbore azimuth angles and perforation phasing angles. There are two extreme cases:

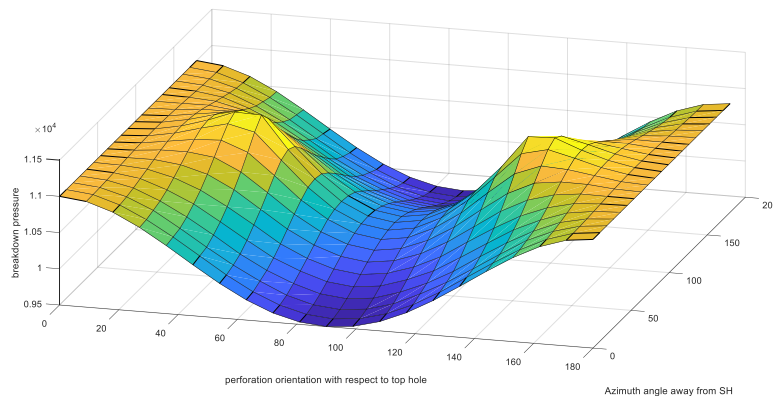


Figure 13: Breakdown pressure distribution for a strike-slip faulting stress regime

1. Minimum breakdown for a well with side perforations (90 degree perforation phasing angle) and SH wellbore orientation (0 degree azimuth angle)

At this orientation, SH and SV are the stresses acting on the perforation wall, the breakdown pressure is calculated as follows:

$$P_b = 3 * S_V - S_H + T_0 \quad (12)$$

- Maximum breakdown for a well with 45 degree perforation phasing angle for a wellbore oriented towards Sh (90 degree wellbore azimuth angle)

Fig. 14 shows the breakdown pressure distribution for different perforation phasing angle. The range of breakdown pressure distribution defines the angle around perforation. The minimum breakdown pressure maximizes at around 45 degrees. This is the maximum breakdown pressure for all azimuth angles.

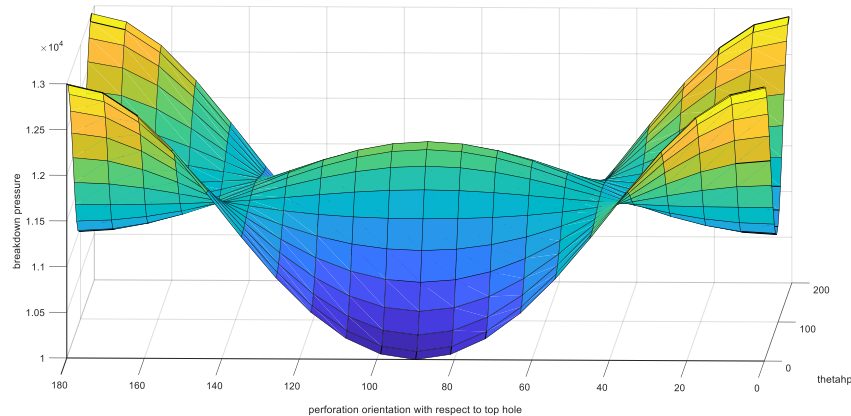


Figure 14: Maximum breakdown pressure case for reverse faulting stress regime

CONCLUSIONS

Unconventional shale reservoirs are extremely tight and under high in-situ stresses. Depending on the in-situ stress magnitudes and the faulting stress regime, shale reservoirs require large surface pumping horsepower to break down the formation but often breakdown cannot be achieved. Therefore, an accurate calculation of breakdown pressure is required to select the optimum surface and downhole completion design in order to achieve breakdown. Several models were developed to calculate the breakdown pressure. This paper reviewed these models and adopted some concepts to build a new model.

The results from the developed model recommend deep penetration depths to expose the perforation tunnels to far field in-situ stresses. Also, different faulting stress regimes are considered. For normal faulting stress regimes, the results from the model predict the lowest breakdown pressure for a wellbore aligned with minimum horizontal stress, a typical wellbore orientation for shale reservoirs. Therefore, it is recommended to steer the drilling bit as close as possible to Sh azimuth. It is also recommended to orient perforations on the sides of the wellbore to achieve lowest breakdown pressures. For wellbores oriented towards the maximum horizontal stress, it is recommended to perforate on top/bottom of the wellbore. For strike-slip faulting stress regime, it is recommended to perforate on top/bottom of the wellbore for any wellbore azimuth angles, whereas it is recommended to perforate on the sides of the wellbore for reverse faulting stress regimes.

Oil and gas operators use a phased perforation technique as the local stresses around the perforations are generally unknown. This study recommends using oriented perforations to minimize the formation breakdown pressures. This could result in avoiding excessive surface pumping horsepower and downhole completions, saving well completion and stimulation costs. Future work will focus on the effect of cement on perturbing the local stresses near the perforation tunnels to increase the accuracy of the current model.

ACKNOWLEDGMENTS

The authors would like to thank the University of New South Wales to allow this work to be published and presented.

REFERENCES

- Bradley, W. 1979. Failure of inclined boreholes. *J. Energy Resources Tech*: 101, 232–239.
- Chen, Z. 2016. UNSW PTRL-6028 Practical Well Planning Notes. UNSW Course Notes.
- Fjaer, E., Holt, R. M., Horsrud, P., Raaen, A. M., and Risnes, R. 2008. *Petroleum Related Rock Mechanics*, 2nd Ed. Amsterdam: Elsevier Publications, pp. 145–147.
- Hossain, M., Rahman, M., Rahman, S. 2000. Hydraulic fracture initiation and propagation: roles of wellbore trajectory, perforation and stress regimes. *Journal of Petroleum Science and Engineering*: 27: 129-49.
- Hubbert, M. K., and Willis, D. G. 1957. Mechanics of hydraulic fracturing. *Pet. Trans. AIME*, v. 210, pp. 153-168.

Khan, S., Oparin, M., Tineo, R., & Bentley, D. 2016. Geomechanical Implications on Unconventional Reservoir Fracturing in Saudi Arabia. Presented at Unconventional Resources Technology Conference. doi:10.15530/URTEC-2016-2394963

Li, Z., Zhao, J., Hu, Y., & Ren, L. 2015. A New Model for Predicting Initiation Pressure of Arbitrarily Inclined -Cased Perforated Well in Naturally Fractured Reservoirs. EJGE.

Rickman, R., Mullen, M. J., Petre, J. E., Grieser, W. V., & Kundert, D. 2008. A Practical Use of Shale Petrophysics for Stimulation Design Optimization: All Shale Plays Are Not Clones of the Barnett Shale. Society of Petroleum Engineers. doi:10.2118/115258-MS

Zoback, M. D. 2010. Reservoir Geomechanics, Cambridge University Press.